N79-27012

MINIMUM ALTITUDE-LOSS SOARING IN A SPECIFIED VERTICAL WIND DISTRIBUTION

Bion L. Pierson and Imao Chen
Iowa State University

SUMMARY

Minimum altitude-loss flight of a sailplane through a given vertical wind distribution is discussed. The problem is posed as an optimal control problem, and several numerical solutions are obtained for a sinusoidal wind distribution.

INTRODUCTION

The problem of determining the optimal sailplane trajectory through a prescribed vertical wind distribution for minimum altitude loss is formulated and solved as an optimal control problem. The flight is assumed to take place in a vertical plane over a fixed range, and the rotational or pitch dynamics of the sailplane are neglected. Sailplane lift coefficient serves as the control function in the nonlinear point-mass equations of motion.

For oscillatory vertical wind distributions, this problem belongs to the class of "optimal dolphin soaring" problems. In qualitative terms, these problems exhibit solutions for which the sailplane speed is decreased in upcurrents to prolong the altitude gain and increased in downcurrents to lessen the altitude loss (ref. 1). Earlier solutions to these problems have assumed either piecewise-static flight (equilibrium glide through segments of constant vertical wind--see, for example, reference 2) or quasi-static flight (kinematic equations of motion only--see, for example, references 3 through 6). Thus, the primary distinguishing feature of this paper is the use of the full nonlinear translational equations of motion and the corresponding use of a modern optimal control algorithm for numerical solutions. Additional research on the application of optimal control theory to dynamic sailplane performance problems may be found in references 7 through 9.

PROBLEM FORMULATION

A brief derivation of the equations of motion used here is provided in the Appendix. The basic assumptions are: flight in a vertical plane, uniform gravity acceleration g and atmospheric density ρ, a point-mass sailplane of constant mass m, and vertical wind of magnitude W. If the vertical wind distribution is further assumed to be independent of altitude ($W = W(x)$), then the right-hand sides of the equations of motion do not depend on altitude Y. The altitude equation (10A) can therefore be incorporated into the performance index (altitude loss)

$$J = Y(0) - Y(t_f) = \int_0^{t_f} (-\dot{Y})dt$$

$$= -\int_0^{t_f} (W + V \sin \gamma)dt \qquad (1)$$

and need not be regarded as a differential constraint.

Furthermore, it will be convenient to regard the range X as the independent variable rather than the time t. Since the final range, $X(t_f) = X_f$, is to be specified, this change of variables will result in a fixed "end-time" optimal control problem which is inherently easier to solve than a variable "end-time" problem. The range equation (9A) can also be omitted from consideration as a differential constraint. It must be tacitly assumed, however, that the optimal trajectory will not include any kind of looping maneuver which would result in zero values for V cos γ. Using (9A) then, the performance index (1) becomes

$$J = -\int_0^{X_f} \left[\frac{W + V \sin \gamma}{V \cos \gamma}\right] dX \qquad (2)$$

and the remaining equations of motion, (11A) and (12A), become

$$\frac{dV}{dX} = -\left|\rho V^2 C_D S/(2m) + [(V \cos \gamma)(dW/dX) + g]\sin \gamma\right| /(V \cos \gamma) \qquad (3a)$$

$$\frac{d\gamma}{dX} = \left|\rho V C_L S/(2m) - [\cos \gamma(dW/dX) + g/V]\cos \gamma\right| /(V \cos \gamma) \qquad (3b)$$

respectively.

Finally, the nondimensional quantities

$$x = X/X_f, \quad v = V(gX_f)^{-\frac{1}{2}}, \quad w = W(gX_f)^{-\frac{1}{2}} \qquad (4)$$

are introduced. The resulting optimal control problem may be stated as follows. Find that control function u(x), $0 \leq x \leq 1$, which minimizes the augmented performance index

$$J = -\int_0^1 \left[\frac{v \sin \gamma + w(x)}{v \cos \gamma}\right] dx + K_1^{-1} \int_0^1 [v/v_{stall} - 1]^{-1} dx$$

$$+ K_2^{-1} \int_0^1 [1 - v/v_{max}]^{-1} dx \qquad (5)$$

subject to the second-order dynamic system

$$\frac{dv}{dx} = -[nC_D(u)v^2 + (1 + \dot{w})\sin \gamma]/(v \cos \gamma), \quad v(0) = v_o \qquad (6a)$$

$$\frac{d\gamma}{dx} = [\eta C_L(u)v^2 - (1 + \dot{w})\cos\gamma]/(v^2\cos\gamma), \quad \gamma(0) = \gamma_o \tag{6b}$$

and subject to the terminal state constraints

$$\psi_1 = v(1)/v_o - 1 = 0 \tag{7a}$$

$$\psi_2 = \gamma(1) - \gamma_o = 0 \tag{7b}$$

where $C_D(u) = a_1 + a_2 C_L + a_3 C_L^2$ (8)

$$C_L(u) = C_{L_{max}}(2\sin^2 u - 1) \tag{9}$$

$$\eta = \frac{1}{2}\rho(S/mg)gX_f \tag{10}$$

and where w(x) is the prescribed wind distribution, $\dot{w} = (dw/dx)(dx/dt) = (dw/dx)v\cos\gamma$, and X_f is the fixed range. Minimum altitude-loss equilibrium glide (still air) values are adopted for the fixed and equal initial and terminal state values, v_o and γ_o. Several additional explanatory comments are required.

First, note that minimum (stall) and maximum (flutter) state inequality constraints on the airspeed are enforced using integral interior penalty functions (ref. 10) shown in terms two and three, respectively, of equation (5). Thus, a sequence of optimal control problems (5) - (10) must be solved for specified positive penalty constants K_1 and K_2. The penalty constants are then increased between subproblems. The solution obtained from each subproblem is used as starting data for the subsequent subproblem. The sequence of subproblems is terminated when each penalty function value is sufficiently small.

Secondly, it may be observed that the lift coefficient is bounded via the transformation (9). That is, for any value of the control function u(x), the control inequality constraints

$$-C_{L_{max}} \leq C_L(u) \leq C_{L_{max}} \tag{11}$$

are satisfied where $C_{L_{max}}$ is a specified constant. Also, note that a quadratic drag polar (8) is used. More accurate drag polars may be used instead provided that an analytical relation is available between C_D and C_L. Finally, it should be observed that for a fixed wing loading, the nondimensional aerodynamic parameter η in equation (10) is proportional to the specified terminal range X_f.

This is the basic optimal control problem considered here. A variation of this problem will also be presented later.

NUMERICAL RESULTS

All computations have been performed on coupled IBM 360/65 and Itel AS/5 computers using a FORTRAN IV compiler and double precision arithmetic. The numerical integration of the required differential equations has been performed using a standard fourth-order Runge-Kutta method with 100 fixed uniform integration steps.

The numerical results have been obtained for the case of a sinusoidal wind distribution

$$w(x) = w_A \sin(2\pi x), \quad 0 \leq x \leq 1 \tag{12}$$

and the Nimbus II open-class sailplane using the gradient projection algorithm presented in reference 11. The sinusoidal wind distribution (12) is simply an idealized model of an oscillatory vertical wind which satisfies a "continuity" condition: the integral of w(x) over the fixed range is zero. The values for the coefficients

$$a_1 = 0.009278, \quad a_2 = -0.009652, \quad a_3 = 0.022288 \tag{13}$$

of the quadratic drag polar (8) for the Nimbus II have been obtained from a least-squares fit of data taken from the manufacturer's velocity polar. For standard sea level conditions and a wing loading, mg/S, of (32)(9.81) N/m^2, the aerodynamic parameter in equation (10) is given by $\eta = 0.01916\ X_f$. Additional constant data chosen include: $C_{L_{max}} = 1.4$, $(gX_f)^{\frac{1}{2}}\ v_{stall} = 18$ m/s and $(gX_f)^{\frac{1}{2}}\ v_{max} = 70$ m/s. Finally, in qualitative terms, the gradient projection method is a direct method in the sense that the control function u(x) is changed during each iteration so as to produce both a decrease in the performance index value (eq. (5)) and full satisfaction of the terminal state constraints (eqs.(7)).

Specified Initial State

In this case, the initial and final state are to be held fixed and equal. In particular, the values

$$(gX_f)^{\frac{1}{2}}\ v_o = 28.1676 \text{ m/s and } \gamma_o = -0.019106 \text{ rad} \tag{14}$$

are to be used in equations (6) and (7) and correspond to the minimum altitude-loss equilibrium glide conditions for the Nimbus II in still air with a drag polar given by equations (8) and (13). The vertical wind amplitude is chosen as $(gX_f)^{\frac{1}{2}}\ w_A = 2$ m/s, and a fixed range of 1000 meters is used.

The resulting optimal trajectory and the corresponding optimal lift coefficient distribution are presented in figures 1 and 2, respectively. The optimal flight can be divided into three successive segments: an initial climb, a maximum C_L arc, and a dive followed by a short pull-up. The initial climb is intuitively reasonable since the sailplane must gain as much altitude as

possible while in the initial upcurrent. The maximum C_L arc is a continuation of the first phase and lasts as long as the wind is strong enough to sustain it. The following dive is made to pass through the downcurrent as quickly as possible. The final pull-up is necessary to meet the terminal state constraints (7). The stall speed inequality constraint was active for this solution, but the maximum speed constraint was not.

The minimum altitude loss for this optimal trajectory is only 12.19 m. By comparison, the minimum altitude loss during an equilibrium glide in still air over the same 1000 m range is 19.11 m. This represents a 36% altitude-loss reduction.

Free but Equal Initial and Final States

Here, the initial and final speed and local flight path angle values are no longer specified, but the respective initial and final values are still required to be equal. The gradient projection algorithm, as described in reference 11, can accomodate the addition of the two control parameters $v(0)$ and $\gamma(0)$ representing variable initial states. However, the presence of these same two control parameters in the terminal state constraints necessitates a further modification to the projection operator equations.

Since the optimal trajectories are now being selected from a larger class, additional performance gains are expected. However, for a final range of 1000 m, the minimum altitude loss improves only 1.4%: from 12.19 m to 12.01 m. For comparison purposes, the optimal trajectory is also shown in figure 1. In this case, the optimal trajectory exhibits a higher altitude gain during the climb phase, a longer maximum C_L arc and a lesser altitude loss in the downcurrent when compared with the previous solution. The initial (and final) airspeed has increased approximately 1.2 m/s to 29.384 m/s.

Effects of Wind Amplitude

The initial and final states are again free but equal. For an increased wind amplitude of $(gX_f)^{\frac{1}{2}} w_A = 5$ m/s, a substantial improvement is obtained as may be noted from the optimal trajectory shown in figure 3. A net altitude gain of 5.158 m is now available over the 1000 m course. Clearly, for higher amplitudes of an oscillating vertical wind, more energy can be extracted from the wind to sustain cross-country flight.

Effects of Varying the Fixed Range

The wind amplitude is held fixed at 5 m/s, and free but equal initial and final states are again considered. Changes in the final range X_f affect only the constant aerodynamic parameter η and the characteristic length and time used in the nondimensionalization. Varying X_f is equivalent to varying the frequency of the sinusoidal wind distribution for sustained flights.

Upon reducing X_f from 1000 m to 500 m, a radically different optimal trajectory was obtained. The corresponding optimal trajectory and optimal C_L distribution are shown in figures 4 and 5, respectively, and will be referred to as a Type II solution. In this case, a dive-first climb-later flight pattern is observed. The average speed is much higher, and the net altitude gain is considerably higher than for the earlier Type I trajectory. The net altitude gain of 23.10 m exceeds that achieved on the previous Type I solution for double the range. For the Type II trajectories, the maximum speed inequality constraint is active rather than the stall speed constraint.

By employing the results of previous Type I solutions as starting data, it was possible to also obtain a Type I solution for X_f = 500 m. However, this Type I relative minimum solution yields a net altitude loss of 4.45 m. Thus, at least for relatively small X_f and large W_A, the Type II solution is decidedly superior to Type I solutions. As a matter of conjecture, the Type II solution may cease to exist for sufficiently large final ranges and/or for sufficiently small wind amplitudes. Two additional solutions were also obtained: a Type I solution for X_f = 750 m and a Type II solution for X_f = 625 m.

Effect of Wing Loading

If the nominal wing loading, mg/S, is increased by 15%, the aerodynamic parameter η becomes 0.01666 X_f (see equation (10)). Nothing else is changed. In this case, a Type I solution was obtained for X_f = 1000 m, W_A = 5 m/s and free but equal initial and final states. The resulting optimal trajectory provides a net altitude gain of 1.14 m which is nearly 4 m less than the comparable 5.16 m obtained earlier for the nominal wing loading. Both the optimal trajectories and the optimal lift coefficient histories for the two solutions are very similar.

The key results for the eight optimal solutions presented here are summarized in table I.

CONCLUSIONS AND DISCUSSION

The optimal control problem treated here is of at least moderate difficulty in view of the state variable inequality constraints present. Relatively few numerical solutions are currently available because of the considerable computational effort involved. However, several tentative conclusions emerge from the computational results obtained thus far.

1) For a sinusoidal vertical wind distribution, which serves as a simple model of a zero range-averaged oscillatory wind, substantial altitude savings are available when compared with optimal equilibrium glides in still air. The relative advantage increases for higher wind amplitudes.

2) Equal initial and final state vector elements can be treated as additional control parameters in the optimal control algorithm and therefore varied as part of the optimization process. The additional altitude gains obtained in this case are, however, rather small.

3) For relatively short ranges and high wind amplitude, it is possible to obtain optimal trajectories which exhibit an unexpected "dive first, climb later" maneuver sequence. Optimal trajectories of this second type involve higher speeds and better final altitude gains than the usual "dolphin" style optimal trajectory.

4) As expected, an increase in sailplane wing loading increases the minimum altitude loss when other conditions are held fixed.

The most surprising finding of this study is the apparent existence of two distinct types of extremal solutions at least for restricted ranges of the parameters involved. Clearly, the Type II trajectory deserves further research effort.

There is also a need to obtain results for other wind distributions and to make definitive comparisons with previous optimization studies which do not incorporate the full translational equations of motion. The related problem of minimum-time flight through a given vertical wind distribution for a specified altitude loss is of perhaps even greater interest. Research on this latter problem is currently underway.

REFERENCES

1. Reichmann, H., Cross-Country Soaring (English translation of Streckensegelflug) Thompson Publications, Santa Monica, California, 1978.

2. Meyer, R., "Dolphin-style gliding," Technical Soaring, Vol. 5, No. 1, 1-9, May 1978.

3. Arho, R., "Optimal dolphin soaring as a variational problem," Acta Polytechnica Scandinavica, Mechanical Engineering Series No. 68, 1972.

4. Irving, F. G., "Cloud-street flying," Technical Soaring, Vol. 3, No. 1, 1-8, Winter 1973.

5. Metzger, D. E. and Hedrick, J. K., "Optimal flight paths for soaring flight," Journal of Aircraft, Vol. 12, No. 11, 867-871, December 1975.

6. de Jong, J. L., "The 'optimal-range-velocity-polar', a new theoretical tool for the optimization of sailplane flight trajectories," Memorandum COSOR 77-28, Department of Mathematics, Eindhoven University of Technology, December 1977.

7. Pierson, B. L., "Maximum altitude sailplane winch-launch trajectories," Aeronautical Quarterly, Vol. 28, No. 2, 75-84, May 1977.

8. Pierson, B. L. and de Jong, J. L., "Cross-country sailplane flight as a dynamic optimization problem," International Journal for Numerical Methods in Engineering, Vol. 12, No. 11, 1743-1759, 1978.

9. Genalo, L. J. and Pierson, B. L., "A singular-arc approximation to a dynamic sailplane flight path optimization problem," Engineering Optimization, Vol. 3, No. 4, 175-182, 1978.

10. Lasdon, L. S., Waren, A. D., and Rice, R. K., "An interior penalty function method for inequality constrained optimal control problems," IEEE Transactions on Automatic Control, Vol. AC-12, No. 4, 388-395, August 1967.

11. Pierson, B. L., "Panel flutter optimization by gradient projection," International Journal for Numerical Methods in Engineering, Vol. 9, No. 2, 271-296, 1975.

APPENDIX: DERIVATION OF THE EQUATIONS OF MOTION

The sailplane velocity vector, relative to the surrounding air, is given by (see figure 6)

$$\vec{V} = \dot{\vec{R}} - \vec{W} \tag{1A}$$

where R is the inertial velocity vector for the sailplane, and $\vec{W}^T = [0, W(X,Y)]$ is the deterministic vertical wind distribution. The angle γ shown in figure 6 is the usual flight path angle for the case of no wind. In the inertial (X,Y)-coordinate frame, the translational equations of motion for unpowered flight in a uniform gravity field may be written as

$$m\ddot{\vec{R}} = \vec{L} + \vec{D} + \vec{G} = m(\dot{\vec{V}} + \dot{\vec{W}}) \tag{2A}$$

where $\vec{L}$ and $\vec{D}$ are the usual aerodynamic lift and drag forces, respectively, $\vec{G}$ is the weight force, and m is the constant sailplane mass. Equation (2A) can be rearranged to yield

$$\begin{aligned}\dot{\vec{V}} &= (\vec{L} + \vec{D} + \vec{G})/m - \dot{\vec{W}} \\ &= \vec{L}/m + \vec{D}/m + [0,-g]^T + [0, -\dot{X}(\partial W/\partial X) - \dot{Y}(\partial W/\partial Y)]^T\end{aligned} \tag{3A}$$

where g is the constant gravity acceleration.

Primarily because of the definitions of lift and drag, it is desirable to rewrite equation (3A) with respect to a rotating (ξ,η)-coordinate frame defined by the unit vectors $\hat{e}_\xi$, directed toward $\vec{V}$, and $\hat{e}_\eta$, directed normal to $\vec{V}$ along the lift vector. The inertial time derivative of $\vec{V}$, referred to this rotating frame, is then given by

$$\begin{aligned}\dot{\vec{V}} &= (d\vec{V}/dt)_{(\xi,\eta)} + \vec{\omega} \times \vec{V} \\ &= \dot{V}\,\hat{e}_\xi + (\dot{\gamma}\,\hat{e}_\zeta) \times (V\,\hat{e}_\xi) \\ &= \dot{V}\,\hat{e}_\xi + V\dot{\gamma}\,\hat{e}_\eta\end{aligned} \tag{4A}$$

where $\hat{e}_\zeta = \hat{e}_\xi \times \hat{e}_\eta$. Note that any vector in the plane, say $\vec{A}$, can be expressed in the rotating (ξ,η)-frame using the following rotation matrix.

$$\vec{A} = \begin{bmatrix} A_\xi \\ A_\eta \end{bmatrix} = \begin{bmatrix} \cos\gamma & \sin\gamma \\ -\sin\gamma & \cos\gamma \end{bmatrix} \begin{bmatrix} A_X \\ A_Y \end{bmatrix} \tag{5A}$$

Using equation (5A), one obtains

$$\vec{G}/m - \dot{\vec{W}} = -[\dot{X}(\partial W/\partial X) + \dot{Y}(\partial W/\partial Y) + g][\sin\gamma\,\hat{e}_\xi + \cos\gamma\,\hat{e}_\eta] \tag{6A}$$

The term, $g + \dot{W} = g + \dot{X}(\partial W/\partial X) + \dot{Y}(\partial W/\partial Y)$, is often referred to as the apparent gravity acceleration.

Finally, using equations (4A) and (6A) and the usual expressions for lift and drag, equation (3A) can be written in scalar form as follows.

$$\dot{V} = -\rho V^2 C_D S/(2m) - [\dot{X}(\partial W/\partial X) + \dot{Y}(\partial W/\partial Y) + g]\sin\gamma \tag{7A}$$

$$V\dot{\gamma} = \rho V^2 C_L S/(2m) - [\dot{X}(\partial W/\partial X) + \dot{Y}(\partial W/\partial Y) + g]\cos\gamma \tag{8A}$$

From equation (1A) and the inverse of equation (5A), the kinematic equations may be written as

$$\dot{X} = V\cos\gamma \tag{9A}$$

$$\dot{Y} = W + V\sin\gamma \tag{10A}$$

Therefore, equations (7A) and (8A) beco e

$$\dot{V} = -\rho V^2 C_D S/(2m) - [(V\cos\gamma)(\partial W/\partial X) + (W + V\sin\gamma)(\partial W/\partial Y) + g]\sin\gamma \tag{11A}$$

$$\dot{\gamma} = \rho V C_L S/(2m) - [\cos\gamma(\partial W/\partial X) + (W/V + \sin\gamma)(\partial W/\partial Y) + g/V]\cos\gamma \tag{12A}$$

TABLE I. Summary of Optimal Solutions

TYPE	RANGE m	WIND AMPLITUDE m/s	V(0) = V(1) m/s	$\gamma(0) = \gamma(1)$ rad.	ALTITUDE CHANGE m
I	1000	2	28.168[a]	-0.0191[a]	-12.187
I	1000	2	29.384	0.0511	-12.012
I	1000	5	31.899	-0.0528	5.158
II	500	5	55.011	-0.6286	23.098
II	625	5	53.253	-0.5285	11.283
I	750	5	31.518	-0.0089	-4.454
I	500	5	30.940	0.0039	-4.452
I	1000	5	33.346	0.0903	1.140[b]

[a] fixed boundary conditions

[b] wing loading increased 15%

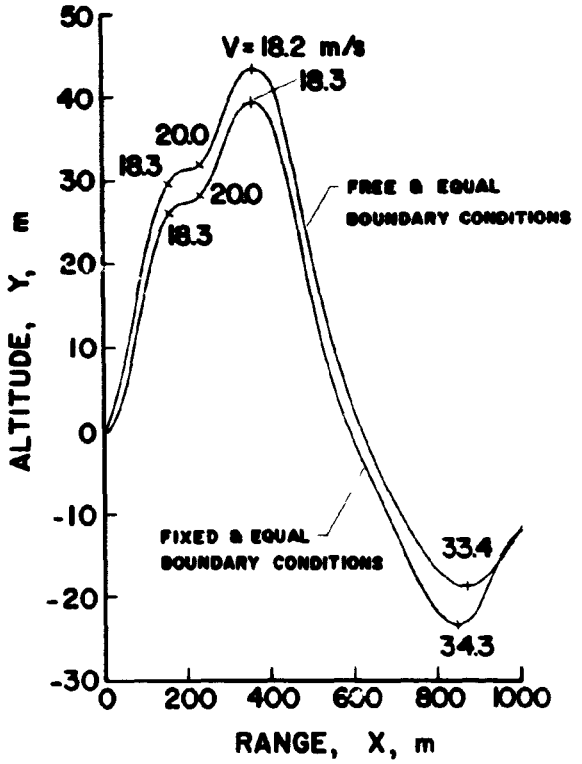

Figure 1.- Optimal trajectories of Type I: W_A = 2 m/s, X_f = 1000 m, V_{stall} = 18 m/s, $C_{L_{max}}$ = 1.4.

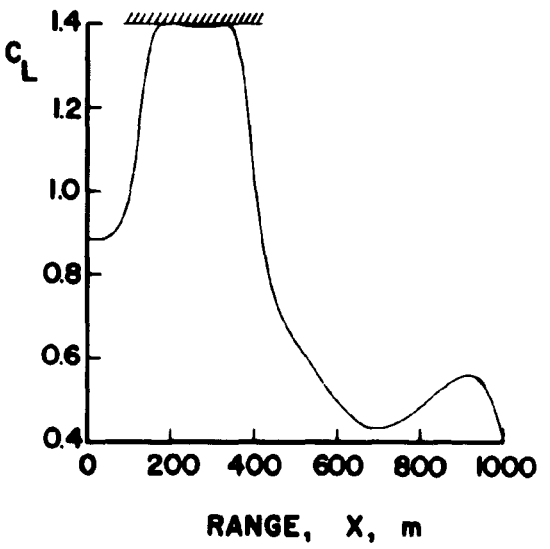

Figure 2.- Optimal lift coefficient distribution for fixed and equal boundary conditions: W_A = 2 m/s, X_f = 1000 m, V_{stall} = 18 m/s, $C_{L_{max}}$ = 1.4.

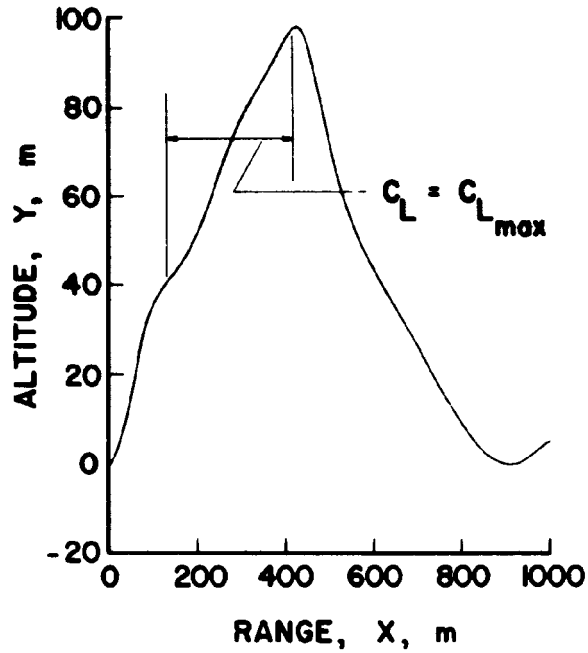

Figure 3.- Optimal Type I trajectory for high wind amplitude: W_A = 5 m/s, X_f = 1000 m, V_{stall} = 18 m/s, $C_{L_{max}}$ = 1.4.

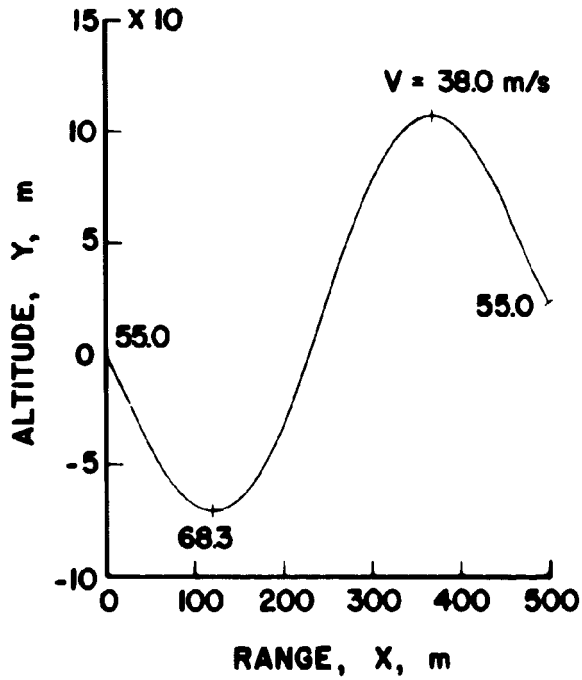

Figure 4.- Optimal Type II trajectory: W_A = 5 m/s, X_f = 500 m, V_{max} = 70 m/s.

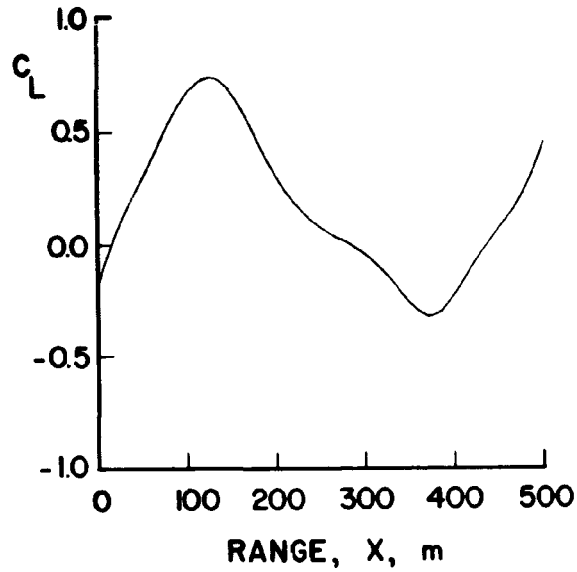

Figure 5.- Optimal lift coefficient distribution for Type II trajectory: W_A = 5 m/s, X_f = 500 m, V_{max} = 70 m/s.

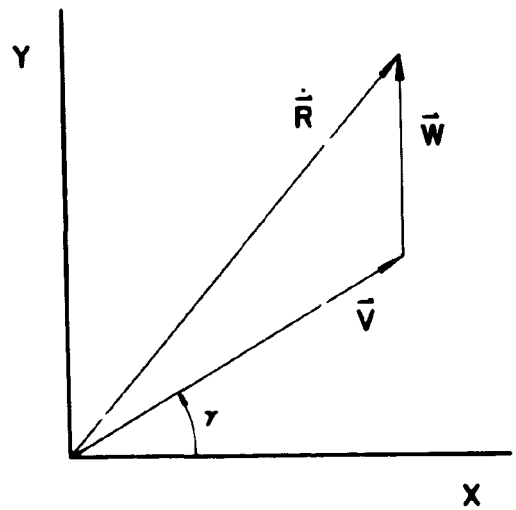

Figure 6.- Velocity vector diagram.